Structural damage detection using auto/cross-correlation functions under multiple unknown excitations

By

Pinghe Ni[1], *Yong Xia*[2,*], *Siu-seong Law*[3], *and Songye Zhu*[4]

Abstract

Traditional structural system identification and damage detection methods use vibration responses under single excitation. This paper presents an auto/cross-correlation function-based method using acceleration responses under multiple ambient white noise or impact excitations. The auto/cross-correlation functions are divided into two parts. One is associated with the structural parameters and the other with the energy of the excitation. These two parts are updated sequentially using a two-stage method. Numerical and experimental studies are conducted to demonstrate the accuracy and robustness of the proposed method. The effects of measurement noise and number of measurement points on the identification results are also studied.

Key words: damage detection, model updating, vibration response, auto/cross-correlation, output-only

---

[1] PhD. student, Department of Civil and Environmental Engineering, The Hong Kong Polytechnic University, Hung Hom, Kowloon, Hong Kong, People's Republic of China

[2] Associate Professor, Department of Civil and Environmental Engineering, The Hong Kong Polytechnic University, Hung Hom, Kowloon, Hong Kong, People's Republic of China.

[3] Professor, Department of Civil and Environmental Engineering, The Hong Kong Polytechnic University, Hung Hom, Kowloon, Hong Kong, People's Republic of China

[4] Assistant Professor, Department of Civil and Environmental Engineering, The Hong Kong Polytechnic University, Hung Hom, Kowloon, Hong Kong, People's Republic of China

[*] Corresponding author: ceyxia@polyu.edu.hk.

1. Introduction

Traditional damage detection methods can be classified into two categories: time domain methods and frequency methods. The basic idea of frequency domain methods is that modal parameters (such as frequencies and mode shapes) are functions of physical parameters. The modal parameters are extracted via modal identification methods[1], and the structural parameters are subsequently identified using model updating techniques[2, 3]. The time domain methods use the measured time history responses directly for damage detection. The error between the calculated dynamic responses (such as acceleration) and measured counterparts is minimized. Several methods, such as quadratic sum-squares error method[4], extended Kalman filter method[5, 6], least-squares method[7], and others[8, 9] have been proposed for damage detection using acceleration responses.

Damage detection methods with unknown input force are more promising for engineering applications because the excitations (for example, wind loading) are usually difficult to measure. Thus, identifying a system that uses the measured responses only without the excitation information would be desirable. However, these methods require that the number of sensors should be larger than the total number of unknown excitations and the measurements (sensors) must be available at the DOFs where the external excitations act[5, 6]. These limitations are the necessary conditions for the existence of the analytical recursive solution[6], which discourages the use of most existing algorithms for a practical structure, and a new method for damage detection without these limitations should be explored.

Recently, damage detection methods to overcome the later limitation have been developed. Yang *et al.*[10] proposed a damage detection method based on the cross-correlation function amplitude vector (CorV) of the measured responses. The damage can be detected and located using the relative difference between CorVs before and after damage. They introduced the inner product vector[11, 12] of cross-correlation function for damage detection. Li and Law[13, 14] proposed a damage detection method based on the covariance of covariance matrix, which is formed from the auto/cross-correlation function of the acceleration responses of the structure under ambient white noise excitation. The covariance of covariance matrix was found more sensitive to local damage than modal frequencies and mode shapes. However, these methods are proposed for damage detection

under single excitation. Practical structures are usually subjected to multiple excitations (for instance, wind loading and traffic loading), and these methods[10-14] fail to identify the structural parameters under multiple unknown excitations. Consequently, methods for system identification and damage detection under multiple unknown excitations are imperative.

In the present paper, an auto/cross-correlation function-based damage detection method is proposed for civil structure under multi-excitations without above mentioned limitations. The auto/cross-correlation function under multiple excitations is derived as two parts. One is associated with the unit impulse response function that depends on structural parameters. The other is a constant part that depends on the energy of the excitation force. The structural parameters are then obtained through the model updating technique. Numerical and experimental studies are performed to demonstrate the effectiveness of the proposed method.

2. Damage detection method

2.1 Cross-correlation function under single excitation

2.1.1 Cross-correlation function of response under white noise excitation

The equation of motion of an N-degree-of-freedom (DOF) damped structural system is given as

$$\boldsymbol{M}\ddot{\boldsymbol{x}}(t)+\boldsymbol{C}\dot{\boldsymbol{x}}(t)+\boldsymbol{K}\boldsymbol{x}(t)=\boldsymbol{B}f(t) \quad , \tag{1}$$

where $\boldsymbol{M}$, $\boldsymbol{C}$, and $\boldsymbol{K}$ are the $N\times N$ mass, damping, and stiffness matrices, respectively; $f(t)$ is the excitation force; and $\boldsymbol{B}$ is the mapping vector with 1 at the excitation location and 0 at others. $\boldsymbol{x}(t)$, $\dot{\boldsymbol{x}}(t)$, and $\ddot{\boldsymbol{x}}(t)$ are the $N\times 1$ displacement, velocity, and acceleration vectors, respectively. Assume that the structure has zero initial conditions and excitation force $f(t)$ is a white noise process.

The acceleration response of the structure at i-th DOF can be expressed as

$$\ddot{x}_i(t)=\int_{-\infty}^{\infty}\ddot{h}_i(t-\tau)f(\tau)d\tau \quad , \tag{2}$$

where $\ddot{h}_i(t)$ is the unit impulse response function at i when the structure is subjected to a unit

impulse force.

Let $R_{ij}(\tau)$ denote the cross-correlation function of the accelerations of at the *i*-th and *j*-th DOFs of the system, which can be written as follows[13, 15]:

$$R_{ij}(\tau) = E\left\{\int_{-\infty}^{t} \ddot{h}_i(t-\mu_1) f(\mu_1) d\mu_1 \times \int_{-\infty}^{t-\tau} \ddot{h}_j(t-\tau-\mu_2) f(\mu_2) d\mu_2\right\}, \tag{3}$$

where μ_1 and μ_2 are the small time variations. With the assumption of white noise excitation, the above equation can be rewritten as

$$R_{ij}(\tau) = \int_{-\infty}^{t}\int_{-\infty}^{t-\tau} \ddot{h}_i(t-\mu_1)\ddot{h}_j(t-\tau-\mu_2) \times E\left(f(\mu_1) f(\mu_2)\right) d\mu_1 d\mu_2 . \tag{4}$$

The auto-correlation function of $f(t)$ is[13, 15]

$$E\left(f(\mu_1) f(\mu_2)\right) = S\delta(\mu_1 - \mu_2) , \tag{5}$$

where *S* is a constant defining the excitation energy and δ is the Dirac delta function.

When $\mu_1 = \mu_2$, Eqs. (4) and (5) give[13]

$$R_{ij}(\tau) = S\int_{0}^{+\infty} \ddot{h}_i(t)\ddot{h}_j(t-\tau) dt . \tag{6}$$

Define

$$\boldsymbol{H}_{ij}(\boldsymbol{\theta}) = \int_{0}^{+\infty} \ddot{h}_i(t)\ddot{h}_j(t-\tau) dt . \tag{7}$$

Eq. (7) is the function of structural physical parameters only. $\boldsymbol{\theta}$ is a vector consisting of the stiffness parameters of each element. Consequently, Eq. (6) can be written as

$$R_{ij}(\tau) = \boldsymbol{H}_{ij}(\boldsymbol{\theta}) S . \tag{8}$$

Eq. (8) indicates that the cross-correlation function depends only on structural parameters $\boldsymbol{H}_{ij}(\boldsymbol{\theta})$ and constant *S*.

2.1.2 Cross-correlation function of response under unit impulse excitation

Instrumented hammers have likewise been widely used in laboratory experiments. The excitation force can be described as a large constant force applied that lasts within a very short time duration as

$$f(t) = \begin{cases} A\delta(t), & 0 \le t \le \varepsilon \\ 0, & else \end{cases} \tag{9}$$

where *A* is a constant, and ε is the impulse duration.

Substituting Eq. (9) into Eq. (2), the acceleration response of the structure can be expressed as

$$\ddot{x}_i(t) = A\int_0^{\infty} \ddot{h}_i(t-\tau)\delta(\tau)\,d\tau \quad . \tag{10}$$

According to the property of Dirac delta function,

$$\ddot{x}_i(t) = A\ddot{h}_i(t) \quad . \tag{11}$$

Therefore, the cross-correlation function R_{ij} can be written as

$$\begin{aligned} R_{ij}(\tau) &= \int_0^{+\infty} \ddot{x}_i(t)\ddot{x}_j(t-\tau)\,dt \\ &= \int_0^{+\infty} A\ddot{h}_i(t)A\ddot{h}_j(t-\tau)\,dt \\ &= A^2\int_0^{+\infty} \ddot{h}_i(t)\ddot{h}_j(t-\tau)\,dt \end{aligned} \quad . \tag{12}$$

The cross-correlation functions under impulse excitation and white noise excitation have a similar form as shown in Eq. (6) and Eq. (12), respectively. The unit impulse response function $\ddot{h}_i(t)$ in both cases can be obtained in Eq. (1), where $f(t)$ is a Dirac delta function. The function can be regarded as a free vibration state with some specific initial conditions. Assuming that the system is initially in static equilibrium, the unit impulse response function can be calculated using the Newmark method[16]:

$$\begin{cases} \boldsymbol{M}\ddot{\boldsymbol{h}}(t) + \boldsymbol{C}\dot{\boldsymbol{h}}(t) + \boldsymbol{K}\boldsymbol{h}(t) = 0 \\ \boldsymbol{h}(0) = 0, \dot{\boldsymbol{h}}(0) = \boldsymbol{M}^{-1}\boldsymbol{B} \end{cases} \quad . \tag{13}$$

where, $\boldsymbol{h}(t)$, $\dot{\boldsymbol{h}}(t)$ and $\ddot{\boldsymbol{h}}(t)$ are the unit impulse displacement, velocity and acceleration vectors, respectively.

2.2 Cross-correlation function under multiple excitations

Previous studies usually considered only single excitations. However, practical structures are generally subjected to external forces at multiple points. Multiple white noise or impulse excitations are investigated in this section. The equation of motion of an *N*- DOF damped structural system under multiple excitations is given as

$$\boldsymbol{M}\ddot{\boldsymbol{x}}(t) + \boldsymbol{C}\dot{\boldsymbol{x}}(t) + \boldsymbol{K}\boldsymbol{x}(t) = \sum_{i=1}^{nf} \boldsymbol{B}_i f_i(t), \tag{14}$$

where f_i is the i-th excitation force, $\boldsymbol{B}_i$ is the mapping vector corresponding to excitation f_i, and nf is the total number of excitations.

The responses under the multiple excitations can be written as the superposition of those under single excitation. That is,

$$\ddot{x}_i(t) = \ddot{x}_{i,1}(t) + \ddot{x}_{i,2}(t) + \cdots \ddot{x}_{i,nf}(t) = \sum_{p=1}^{nf} \ddot{x}_{i,p}(t) \ , \tag{15}$$

where $\ddot{x}_{i,p}(t)$ is the response at the *i*-th DOF under *p*-th single excitation force.

Let $R_{\ddot{x}_i,\ddot{x}_j}(\tau)$ denote the cross-correlation function of the accelerations at the *i*-th and *j*-th DOFs of the system under the multiple excitations. It can be written as

$$R_{\ddot{x}_i,\ddot{x}_j}(\tau) = R_{\left(\ddot{x}_{i,1}+\ddot{x}_{i,2}+\cdots+\ddot{x}_{i,nf}\right),\left(\ddot{x}_{j,1}+\ddot{x}_{j,2}+\cdots+\ddot{x}_{j,nf}\right)}(\tau) = \sum_{p=1}^{nf}\sum_{q=1}^{nf} R_{\ddot{x}_{i,p},\ddot{x}_{j,q}}(\tau) \tag{16}$$

and

$$R_{\ddot{x}_{i,p},\ddot{x}_{j,q}}(\tau) = \int_{-\infty}^{t}\int_{-\infty}^{t-\tau} \ddot{h}_{i,p}(t-\mu_1)\ddot{h}_{j,q}(t-\tau-\mu_2) \times E\left(f_p(\mu_1) f_q(\mu_2)\right) d\mu_1 d\mu_2 , \tag{17}$$

where $\ddot{h}_{i,p}(t)$ is the unit impulse response functions at *i* under excitation at *p* locations.

The excitations are uncorrelated and, consequently, $E\left(f_p(\mu_1) f_q(\mu_2)\right) = 0$ ($p \neq q$). This equation leads to

$$R_{\ddot{x}_{i,p},\ddot{x}_{j,q}}(\tau) = 0 \quad (p \neq q). \tag{18}$$

Therefore, Eq. (16) can be expressed as

$$R_{\ddot{x}_i,\ddot{x}_j}(\tau) = \sum_{p=1}^{nf} R_{\ddot{x}_{i,p},\ddot{x}_{j,p}}(\tau) \ . \tag{19}$$

As discussed in section 2.1.1, the auto-correlation function of $f_p(t)$ is

$$E\left(f_p(\mu_1) f_p(\mu_2)\right) = S_p \delta(\mu_1 - \mu_2) . \tag{20}$$

Then,

$$R_{\ddot{x}_{i,p},\ddot{x}_{j,p}}(\tau) = S_p \int_0^{+\infty} \ddot{h}_{i,p}(t), \ddot{h}_{j,p}(t-\tau)\, dt \ . \tag{21}$$

Define

$$\boldsymbol{H}(\boldsymbol{\theta}) = \left[\boldsymbol{H}_1, \boldsymbol{H}_2, \cdots \boldsymbol{H}_p, \cdots \boldsymbol{H}_{nf}\right] \quad , \tag{22}$$

$$\boldsymbol{H}_p = \int_0^{+\infty} \ddot{h}_{i,p}(t)\ddot{h}_{j,p}(t-\tau)\, dt \quad , \tag{23}$$

$$\boldsymbol{s} = \left[S_1, S_2, \cdots, S_p \cdots, S_{nf}\right]^T \quad . \tag{24}$$

The cross-correlation function between different sensors can be rewritten as

$$\boldsymbol{R}(\tau) = \boldsymbol{H}(\boldsymbol{\theta})\boldsymbol{s} = \boldsymbol{R}(\boldsymbol{\theta}, \boldsymbol{s}) \ . \tag{25}$$

In Eq. (23), $\ddot{h}_{i,p}(t)$ and $\ddot{h}_{j,p}(t)$ can be obtained in a similar manner as that under a single

excitation. In practice, the cross-correlation function of acceleration can be obtained as a discrete inverse Fourier transform of the cross-spectral density function[17].

The above section shows that the cross-correlation function of acceleration responses, regardless of whether single or multiple excitations, can be written as the product of a constant and a function of structural parameters. A damage detection method based on the cross-correlation function is proposed in the following section.

2.3 Damage detection using cross-correlation function

Assuming that the structural damage is in the form of a change in the structural stiffness, the stiffness matrix of the damaged structure can then be expressed as

$$\boldsymbol{K}^{d} = \sum_{i=1}^{ne} \theta_i K_i \quad , \tag{26}$$

where K_i is the stiffness matrix of the *i*-th element in the intact state, θ_i ($0 \le \theta_i \le 1$) is defined as the stiffness fraction to the intact stiffness of the *i*-th element, and ne is the total number of elements in the structure. $\theta = 0$ denotes that the element loses its stiffness completely, whereas $\theta = 1$ indicates that the element is intact.

The problem of system identification is to determine the system parameters $\boldsymbol{\theta}$ from the measured cross-correlation function using the model updating technique[18]. The objective function for model updating is defined as the difference between the measured and calculated cross-correlation functions

$$\boldsymbol{J} = \left\| \boldsymbol{R}_{mea} - \boldsymbol{R}_{cal} \right\| \quad , \tag{27}$$

where $\boldsymbol{R}_{mea}$ is the measured cross-correlation function and $\boldsymbol{R}_{cal}$ is the corresponding cross-correlation function calculated from the finite element model.

A two-stage method is employed in model updating. In the first stage, constant coefficient part $\boldsymbol{s}$ can be estimated from Eq. (25) as

$$\boldsymbol{s} = \boldsymbol{H}\left(\boldsymbol{\theta}\right)^{+} \boldsymbol{R}_{mea} \tag{28}$$

given the initial value of $\boldsymbol{\theta}$, where $\boldsymbol{H}\left(\boldsymbol{\theta}\right)^{+}$ is the pseudo-inverse of $\boldsymbol{H}\left(\boldsymbol{\theta}\right)$.

In the second stage, the cross-correlation function can be expressed as a first-order Taylor expansion[18]

$$\Delta \boldsymbol{R} = \boldsymbol{R}_{mea} - \boldsymbol{R}_{cal} = \frac{\partial \boldsymbol{R}_{cal}}{\partial \boldsymbol{\theta}} \Delta \boldsymbol{\theta} + o(\boldsymbol{\theta}^2) \tag{29}$$

$$\frac{\partial \boldsymbol{R}_{cal}}{\partial \boldsymbol{\theta}} = \left[\frac{\partial \boldsymbol{R}_{cal}}{\partial \theta_1}, \frac{\partial \boldsymbol{R}_{cal}}{\partial \theta_2}, \cdots \frac{\partial \boldsymbol{R}_{cal}}{\partial \theta_i}, \cdots \frac{\partial \boldsymbol{R}_{cal}}{\partial \theta_{ne}} \right] \quad . \tag{30}$$

The high order terms $o(\boldsymbol{\theta}^2)$ are small and can be ignored. $\frac{\partial \boldsymbol{R}_{cal}}{\partial \boldsymbol{\theta}}$ is the sensitivity matrix of the cross-correlation function with respect to structural parameters, which can be obtained using the Newmark method[13] or the forward difference method[19] as

$$\begin{aligned} \frac{\partial \boldsymbol{R}_{cal}}{\partial \theta_i} &= \lim_{\varphi \to 0} \frac{\boldsymbol{R}_{cal}\left(\left[\theta_1, \theta_2, \cdots, \theta_i + \varphi, \cdots \theta_{ne}\right], \boldsymbol{s}\right) - \boldsymbol{R}_{cal}\left(\left[\theta_1, \theta_2, \cdots, \theta_i, \cdots \theta_{ne}\right], \boldsymbol{s}\right)}{\varphi} \\ &= \frac{\boldsymbol{R}_{cal}\left(\left[\theta_1, \theta_2, \cdots, \theta_i + \varphi, \cdots \theta_{ne}\right], \boldsymbol{s}\right) - \boldsymbol{R}_{cal}\left(\left[\theta_1, \theta_2, \cdots, \theta_i, \cdots \theta_{ne}\right], \boldsymbol{s}\right)}{\varphi} \end{aligned} \quad . \tag{31}$$

where φ is the incremental step for the finite difference method.

Eq. (29) can be solved by the damped least-squares method as

$$\Delta \boldsymbol{\theta} = \left[\left(\frac{\partial \boldsymbol{R}_{cal}}{\partial \boldsymbol{\theta}} \right)^T \left(\frac{\partial \boldsymbol{R}_{cal}}{\partial \boldsymbol{\theta}} \right) + \boldsymbol{\lambda} \right]^{-1} \left(\frac{\partial \boldsymbol{R}_{cal}}{\partial \boldsymbol{\theta}} \right)^T \Delta \boldsymbol{R} \quad , \tag{32}$$

where $\boldsymbol{\lambda}$ is the non-negative optimal regularization parameter determined by the L-curve method[20].

Structural parameters $\boldsymbol{\theta}$ in the undamaged state can be obtained using the model updating technique. Similarly, those in the damaged state $\tilde{\boldsymbol{\theta}}$ can be obtained when measured accelerations are available. The structural damage can be identified as

$$\alpha_i = \frac{\tilde{\theta}_i - \theta_i}{\theta_i} \quad . \tag{33}$$

The nonzero value of α_i denotes the damage at element *i*.

2.4 Implementation Procedures

The above cross-correlation-based damage detection procedure can be summarized as follows:

Step 1: Measure the structural responses under ambient white noise excitations or impulse excitations and calculate the auto/cross-correlation functions.

Step 2: Set the initial value of the structural parameter $\boldsymbol{\theta}^0 = \left[\theta_1^0, \theta_2^0, \cdots, \theta_{ne}^0\right]$.

Step 3: Calculate $\boldsymbol{H}(\boldsymbol{\theta})$ from Eq. (22) and estimate constant value $\boldsymbol{s}$ from Eq. (28).

Step 4: Calculate the auto/cross-correlation function from Eq. (25) and the sensitivity matrix from

Eq. (31).

Step 5: Update the structural parameters from $\boldsymbol{\theta}^{i+1} = \boldsymbol{\theta}^{i} + \Delta\boldsymbol{\theta}$, where $\Delta\boldsymbol{\theta}$ is obtained from Eq. (32).

Step 6: Repeat steps 3 to 5 until the following convergence condition in Eq. (34) is satisfied. The tolerance in this paper is set to 10^{-5}.

$$\frac{\left\|\boldsymbol{\theta}^{i+1} - \boldsymbol{\theta}^{i}\right\|}{\left\|\boldsymbol{\theta}^{i}\right\|} \times 100\% < \ Tolerance \tag{34}$$

Step 7: For damage detection, the measurement responses before and after damage are both available. The stiffness parameters $\boldsymbol{\theta}$ and $\tilde{\boldsymbol{\theta}}$ can be identified, respectively.

Step 8: Compare the changes in element stiffness with Eq. (33) to identify the elements of the damages.

3. Numerical study

The steel cantilever beam[21] shown in Figure 1 was used for the numerical study. The size of the cross-section was 50.75 mm×6.0 mm, and the mass density was 7.67×10^{3} kg/m^{3}. The structure was modeled with nine Euler–Bernoulli beam elements (i.e., *ne*=9). The initial Young's modulus in the intact state was 2.0×10^{11} N/m^{2}.

The structure was subjected to two white noise excitations in the vertical direction, as shown in Figure 1, with a zero mean and unit standard deviation. The computed responses from Eq. (1) under the excitation are taken as the "measured" responses for the following studies. The sampling frequency was 2000 Hz and 3 h force vibration responses were recorded. The calculated acceleration responses in the vertical direction were considered as the "measured" responses. The auto/cross-correlation function was calculated from the measured responses, and the first 100 data of auto/cross-correlation function were selected for the numerical study.

3.1 Structural stiffness identification

The real elastic modulus of the structural material is simulated by adding a random variation to the initial ones (i.e., 2.0×10^{11} N/m^{2}). The random variation has a normal distribution, with 10% standard deviation of its initial value. Since the acceleration responses are calculated, the

cross-spectral density function of the response can be obtained. Then the cross-correlation function of acceleration can be obtained as a discrete inverse Fourier transform of the cross-spectral density function[17]. The cross-correlation function of accelerations at Nodes 4 and 6 ($\boldsymbol{R}_{4,6}$) was used for system identification.

The real stiffness parameter of each element was identified using the proposed two-stage model updating technique. The initial values of the stiffness factors for iteration were set the same at 1.2, as shown in Figure 2. The model updating results converge approximately after 40 iterations. The final identified stiffness factors highly agree with the true values without any false alarm, as shown in Figure 3. The maximum relative error between the true value and the identification result is 1.0 % at Element 1.

3.2 Effect of measurement noise

Random noise is added to the measured response to simulate the uncertainty of the measurements as

$$\ddot{\boldsymbol{x}}^m = \ddot{\boldsymbol{x}} + E_p \boldsymbol{N}_{noise} \sigma\left(\ddot{\boldsymbol{x}}\right), \tag{35}$$

where E_p is the percentage noise level, $\boldsymbol{N}_{noise}$ is the standard normal distribution vector with zero mean and unit standard deviation, and $\sigma\left(\ddot{\boldsymbol{x}}\right)$ is the standard deviation of the "measured" acceleration response.

The 10% and 20% measurement noise are respectively added to the "measured" responses to study the effect of measurement noise on the identification results. Figure 4 shows the identified stiffness fractions under different noise levels. The maximum relative error was 1.1% at Element 2 for the case of 10% noise and 2.7% at Element 9 for the case of 20% noise. The results are satisfactory even when 20% noise is included. The effect of the measurement noise is analyzed as follows.

The cross-correlation function of noised responses at *i* and *j* locations can be expressed as

$$\begin{aligned} \boldsymbol{R}_{\ddot{x}_i^m,\ddot{x}_j^m}\left(\tau\right) &= \boldsymbol{R}_{\left(\ddot{x}_i+N_{noise,i}\right),\left(\ddot{x}_j+N_{noise,j}\right)}\left(\tau\right) \\ &= \boldsymbol{R}_{\ddot{x}_i,\ddot{x}_j}\left(\tau\right) + \boldsymbol{R}_{\ddot{x}_i,N_{noise,j}}\left(\tau\right) + \boldsymbol{R}_{N_{noise,i},\ddot{x}_j}\left(\tau\right) + \boldsymbol{R}_{N_{noise,i},N_{noise,j}}\left(\tau\right) \end{aligned}. \tag{36}$$

For white noise that leads to $\boldsymbol{R}_{\ddot{x}_i,N_{noise,j}}\left(\tau\right)=0$ and $\boldsymbol{R}_{N_{noise,i},\ddot{x}_j}\left(\tau\right)=0$,

$$\boldsymbol{R}_{\ddot{x}_i^m,\ddot{x}_j^m}\left(\tau\right) = \begin{cases} \boldsymbol{R}_{\ddot{x}_i,\ddot{x}_j}\left(\tau\right) \ (i \neq j) \\ \boldsymbol{R}_{\ddot{x}_i,\ddot{x}_j}\left(\tau\right) + \left(E_p\sigma\right)^2 \delta\left(\tau\right) \ (i = j) \end{cases}. \tag{37}$$

In theory, the cross-correlation function is noise free, and the auto-correlation function contains noise only when $\tau = 0$. Thus, the effect of measurement noise on the system identification results is very small as shown in Figure 5, where the cross-correlation functions of $\boldsymbol{R}_{4,6}$ with 20% noise and without noise are almost identical.

3.3 Effect of less sensor with different sensor location

Two sensors were used for structural parameter identification in Sections 3.1 and 3.2 and the accuracy of the proposed method has been demonstrated. A reduced number of sensors would result in a loss of damage information in the measured responses, which may have a negative effect on the identification results. To study the effect of sensor number and sensor location, only one sensor is used for model updating here.

The excitation force and structural parameters used in Section 3.1 remain unchanged. The auto-correlation function of the vertical acceleration at different sensor points is employed for system identification. The identification errors of each element with respect to different sensor location are shown in Figure 6. It can be found that when the sensor is installed at Node 3, the maximum identification error is 1.8% at Element 1. The identification errors for all cases are small and the maximum relative error is 2.3% at Element 6 when the auto-correlation function at Node 8 is used. The effect of sensor location on the identification results is not significant and the proposed system identification technique is robust.

In this example, the structure is excited under two unknown forces. The present method can identify the structural parameters using one sensor only. This cannot be achieved using the traditional methods, which requires that the number of sensors should be larger than the total number of unknown excitations and the measurements must be available at the DOFs where the external excitations act on[5, 6].

4. Experimental study

Figure 7 shows the constructed steel shear-type four-story building model. The dimensions of the frame are shown in Figure 8. The height of each floor was 300 mm, and the floor of each story was composed of 25 mm thick steel plates. The two columns of each story have the same section shape with a width of 50 mm and a thickness of 5 mm. The beams and columns were welded together to form rigid joints. The bottom of the columns was welded onto a thick and solid steel plate, which was

fixed to the strong floor. The elastic modulus of the steel was estimated to be 200 GPa, and the mass density was 7850 kg/m^3.

4.1 Experimental setup

A SINOCERA LC-04A hammer with a rubber tip was used to excite the frame. Horizontal acceleration responses of the frame were measured at each floor using KD1300 accelerometers. A commercial data logging system INV306U and its associated signal analysis package DASP V10 were used for data acquisition. The sampling frequency was 1024 Hz, and the cut-off frequency range was preset at 1 Hz to 300 Hz for all test cases.

4.2 Modal testing and model updating in the undamaged state

The test was performed by using the hammer to hit the top floor of the frame. In each test, only output time history were recorded for 60 s. Typical curves of auto/cross-correlation functions ($\boldsymbol{R}_{22}$ and $\boldsymbol{R}_{21}$) are displayed in Figure 9. Note that the input time history is for modal analysis only and not necessarily for model updating in the present method.

The first four natural frequencies of the undamaged structure were extracted from the measured input and output using modal analysis. The results are listed in Table 1 along with the results calculated from the numerical model. In the numerical model, the stiffness of each floor was calculated from the physical configuration and material properties of the model, as listed in Table 2. The mass of columns, beams, and sensors were combined for each floor. The calculated mass results were 13.1280, 13.0976, 13.0838, and 12.4948 kg for the first, second, third, and fourth floors, respectively. The analytical frequencies were very close to the measured counterparts. Thus, the model is accurate enough for subsequent model updating. The measured four damping ratios that were obtained from DIAMOND[22] were $\xi_1 = 0.740\%$, $\xi_2 = 0.41\%$, $\xi_3 = 0.34\%$, and $\xi_4 = 0.27\%$, respectively.

The correlation function between the measurement responses for the first to the fourth floors and that at the second floor ($\boldsymbol{R}_{2,1}$, $\boldsymbol{R}_{2,2}$, $\boldsymbol{R}_{2,3}$, and $\boldsymbol{R}_{2,4}$) were used for the initial model updating. The acceleration responses were transformed into auto/cross-correlation functions, and the first 100 data were employed for model updating. The updated stiffness parameters are very close to the initial

values listed in Table 2.

4.3 Damage detection

After performing the dynamic test on the intact frame structure, artificial damage was introduced by reducing the width of two columns in the second floor from 50 mm to 30 mm, as shown in Figure 10. The frame was tested in a similar manner as in the undamaged state. The auto/cross-correlation functions ($\boldsymbol{R}_{2,1}$, $\boldsymbol{R}_{2,2}$, $\boldsymbol{R}_{2,3}$, and $\boldsymbol{R}_{2,4}$) are used to update the model in the damaged state. The identified stiffness parameters in Section 4.2 are used as the initial model for damage detection. The iteration process converges approximately after 10 runs, as shown in Figure 11.

The updated stiffness parameters are shown in Table 2. The stiffness parameter of the second floor is reduced by 41.37% from 124.75 kN/m to 73.14 kN/m, which is very close to the real damage (40% stiffness reduction of the column in the second floor). The other parameters almost remain the same as those before the damage was introduced. The small identification errors of the undamaged elements (less than 5%) may be due to the measurement noise[23-25]. Therefore, both damage location and damage severity are correctly detected. These results demonstrate the accuracy of the proposed method.

5. Conclusions

This paper proposes a damage detection method based on the auto/cross-correlation function of acceleration responses when a structure is subjected to multiple white noise or impulse excitations. The damage is detected by minimizing the error between the measured auto/cross-correlation functions and the calculated counterparts. Numerical and experimental examples were used to demonstrate the effectiveness and robustness of the proposed technique. The advantages of the present method include the following features.

i) The present paper proposes a damage detection method for civil engineering structures under multiple excitations. Previous methods for multiple excitations are rare.

ii) The method uses the response data only (or output only).

iii) The proposed method is robust and insensitive to measurement noise.

iv) The proposed method does not require sensor numbers larger than the number of excitations, as required in other methods[5-7, 16].

Acknowledgements

The authors gratefully acknowledge the financial support provided by the Hong Kong Polytechnic University Research Grant (Project Nos. G-YK74 and 4-ZZCF).

References

1. J. Juang and R. Pappa, An Eigen-system Realization Algorithm for modal parameters identification and model reduction, J. Guid. Control Dynam., 8 (5) (1985) 620-627.
2. S. Weng, Y. Xia, X. Q. Zhou, Y. L. Xu, and H. P. Zhu, Inverse substructure method for model updating of structures, J. Sound Vib., 331 (25) (2012), 5449-5468.
3. S. Weng, Y. Xia, Y. L. Xu, and H. P. Zhu, Substructuring approach to finite element model updating, Comput. Strcut., 89 (9-10) (2012), 772-782.
4. J. N. Yang, H. Huang, and S. W. Pan, Adaptive quadratic sum-squares error for structural damage identification, J. Eng. Mech., ASCE 135 (2009) 67–77.
5. J. N. Yang, S. W. Pan, and H. W. Huang, An adaptive extended Kalman filter for structural damage identification II: unknown inputs, Struct. Control Hlth., 14 (2007) 497-521.
6. Y. Lei, Y. Jiang, and Z. Xu, Structural damage detection with limited input and output measurement signals, Mech. Syst. Signal Pr., 28 (2012) 229-243.
7. J. N. Yang, S. W. Pan, S. Lin, Least square estimation with unknown excitations for damage identification of structures, J. Eng. Mech., ASCE, 133 (2007) 12–21.
8. H. N. Li, T. H. Yi, M. Gu, and L. S. Huo, Evaluation of earthquake-induced structural damages by wavelet transform. Prog. Nat. Sci., 19 (4) (2009), 461-470.
9. Y. T. Hua, H. N. Li, and H. M. Sun, Multi-stage structural damage diagnosis method based on “energy-damage” theory. Smart Struct. Syst. 12 (3-4) (2012), 345-361.
10. Z. C. Yang, Z. F. Yu, and H. Sun, On the cross-correlation function amplitude vector and its application to structural damage detection, Mech. Syst. Signal Pr., 21 (2007) 2918–2932.
11. Z. C. Yang, L. Wang, H. Wang, Y. Ding, and X.J. Dang, Damage detection in composite structures using vibration response under stochastic excitation, J. Sound Vib., 325 (2009)

755–768.

12. L. Wang, Z. C. Yang, and T. P. Waters, Structural damage detection using cross-correlation functions of vibration response, J. Sound Vib., 329 (2010) 5070–5086.
13. X. Y. Li, and S. S. Law, Condition assessment of structures under ambient white noise excitation, AIAA J., 46 (2008) 1395-1404.
14. X. Y. Li, and S. S. Law, Matrix of the covariance of covariance of acceleration responses for damage detection from ambient vibration measurements, Mech. Syst. Signal Pr., 24 (2010) 945-956.
15. J. S. Bendat and A. G. Piersol, Engineering applications of correlation and spectral analysis, Wiley, New York (1980).
16. J. Li, S. S. Law, and H. Hao, Improved damage identification in bridge structures subject to moving loads: numerical and experimental studies, Int. J. Mech. Sci., 74 (2013) 99-111.
17. J. Caicedo, S. Dyke, and E. Johnson, Natural excitation technique and eigensystem realization algorithm for phase I of the IASC-ASCE Benchmark Problem: simulated data, J. Eng. Mech., ASCE, 130(1) (2004) 49–60.
18. Z. R. Lu and S. S. Law, Identification of system parameters and input force from output only, Mech. Syst. Signal Pr., 21(5) (2007) 2099-2111.
19. K. W. Morton and D. F. Mayers, Numerical solution of partial differential equations: an introduction, Cambridge University Press, (2005).
20. A. N. Tikhonov, Numerical methods for the solution of ill-posed problems, Kluwer Academic, Norwell, MA (1995).
21. H. Hao and Y. Xia, Vibration-based damage detection of structures by genetic algorithm, J. Comput. Civil Eng. ASCE, 16 (3) (2002) 222-229.
22. S. W. Doebling, C. A. Farrar, and P. J. Cornwell. DIAMOND: A graphical interface toolbox for comparative modal analysis and damage identification. No. LA-UR--97-38; CONF-970736--2. Los Alamos National Lab., NM (United States), 1997.
23. J. Zhang, Y. L. Xu, Y. Xia, and J. Li, A New Statistical Moment-Based Structural Damage Detection Method. Structural Engineering and Mechanics, 30 (4) (2008), 445-466.
24. Y. L. Xu, J. Zhang, J. C. Li, and Y. Xia, Experimental Investigation on Statistical Moment-based Structural Damage Detection Method., Structural Health Monitoring, 8 (6) (2009), 555-571.

25. L. D. Goh, N. Bakhary, A. A., Rahman, and B. H. Ahmad, Application of Neural Network for Prediction of Unmeasured Mode Shape in Damage Detection, Advances in Structural Engineering, 16 (1) (2013), 99-113.

List of figures and tables

Table 1 Frequencies of the structure in the undamaged state

Mode No.	Calculated (Hz)	Measured (Hz)	Relative Error (%)
1st	5.18	5.17	0.19
2nd	15.01	15.05	-0.27
3rd	23.19	23.52	-1.42
4th	28.60	29.20	-2.10

Table 2 Column flexural stiffness

Story No.	Initial value (kN/m)	Identified result before damage (kN/m) θ	Identified result after damage (kN/m) $\tilde{\theta}$	Stiffness reduction percentage (%) α
1st	104.66	102.99	107.95	-4.8
2nd	122.21	124.75	73.14	41.4
3rd	122.21	130.16	133.18	-2.3
4th	122.21	117.30	116.83	0.4

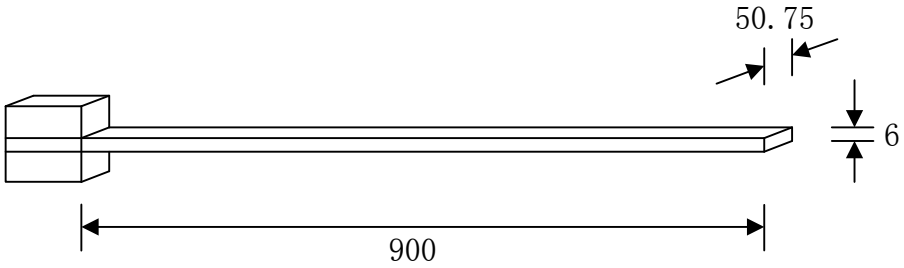

(a) Configuration of the beam specimen (unit: mm)

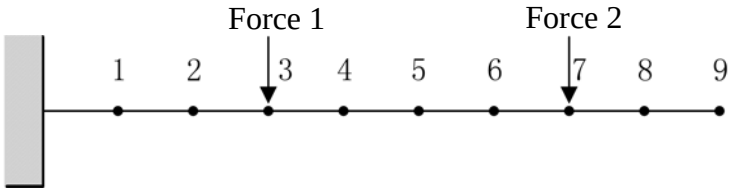

(b) Finite element model of the cantilever beam

Figure 1 Cantilever beam

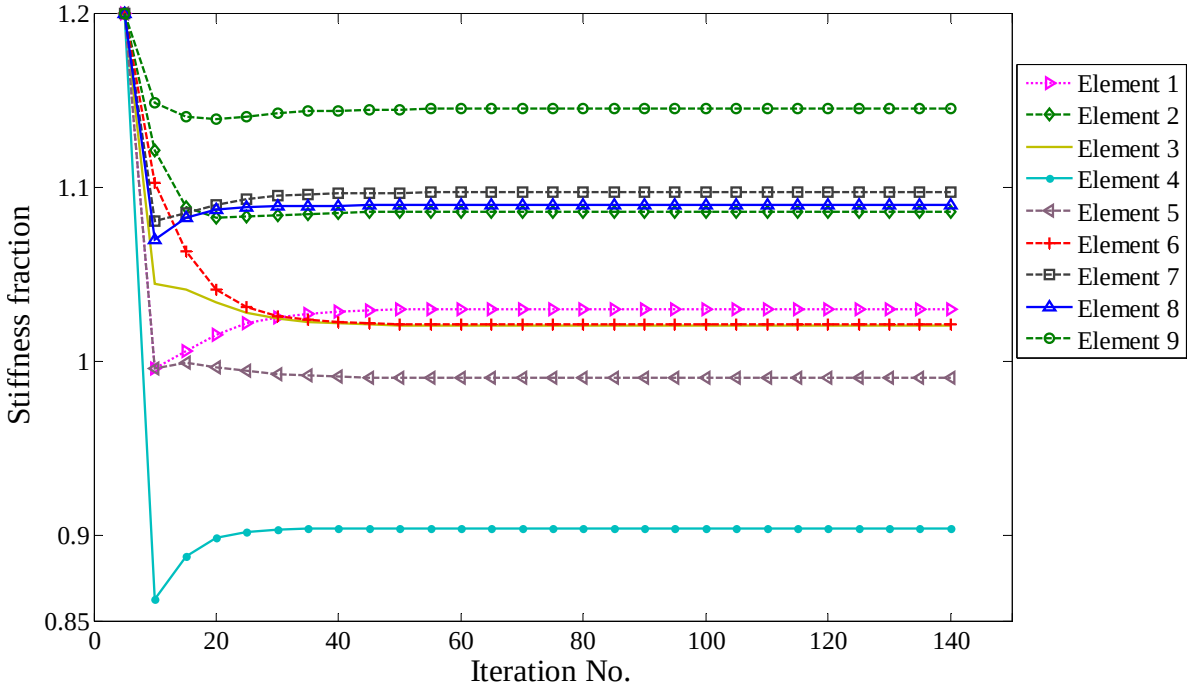

Figure 2 Evolution of identification results of the cantilever beam

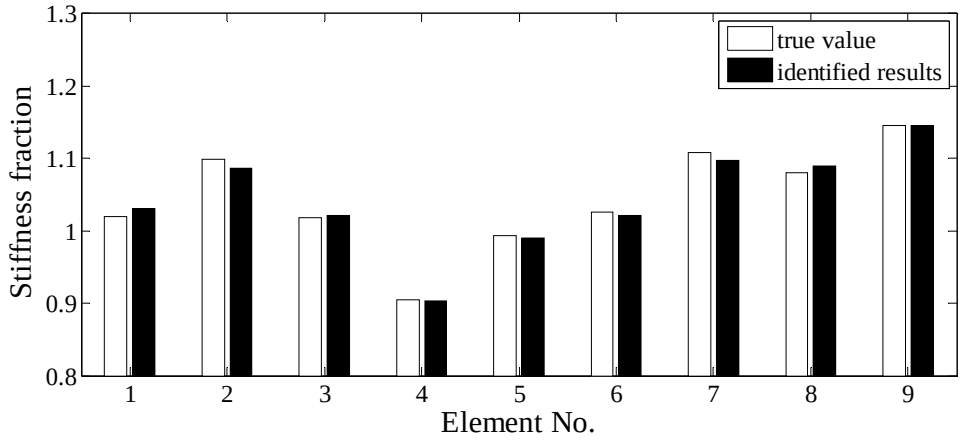

Figure 3 Model updating results without measurement noise

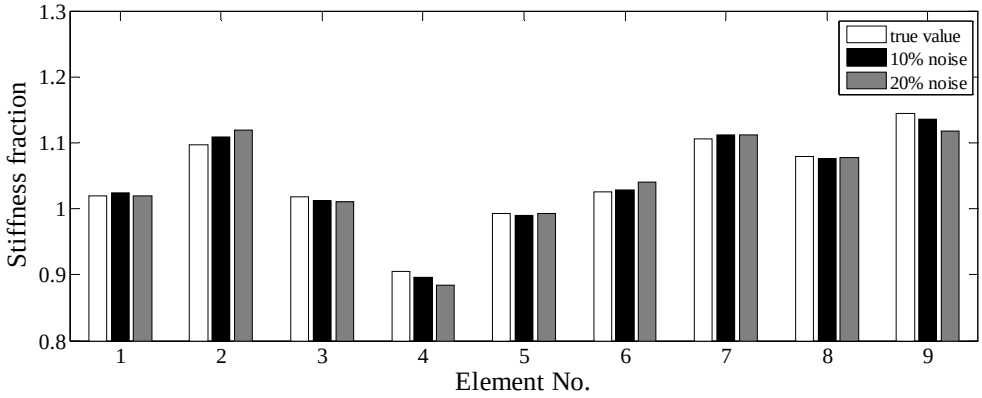

Figure 4 Model updating results with different noise levels

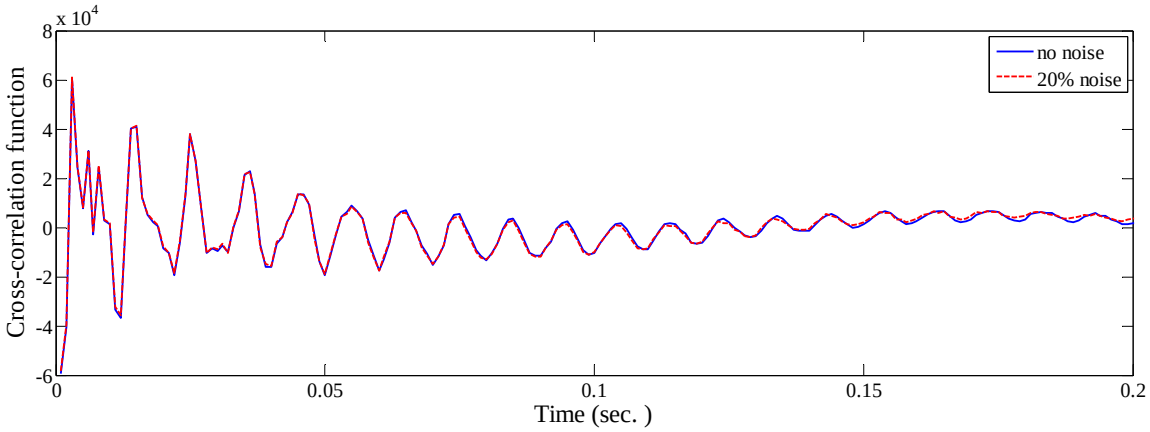

Figure 5 Comparison between the cross-correlation functions $\boldsymbol{R}_{4,6}$ with and without measurement noise

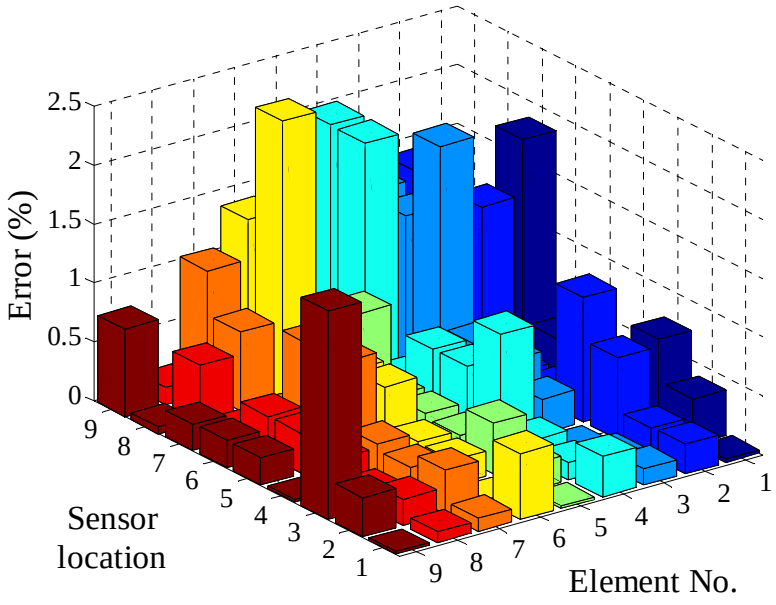

Figure 6 Identification error from different sensor locations

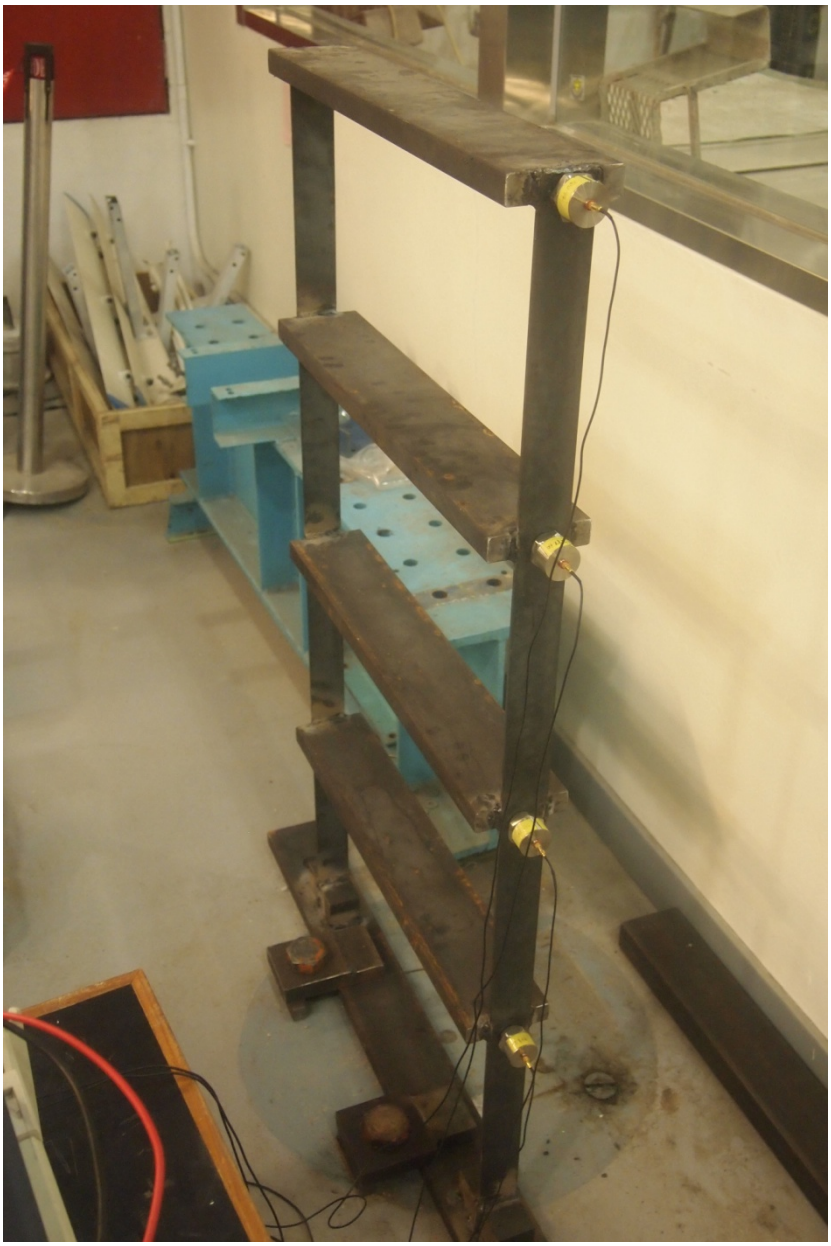

Figure 7 Laboratory steel frame model

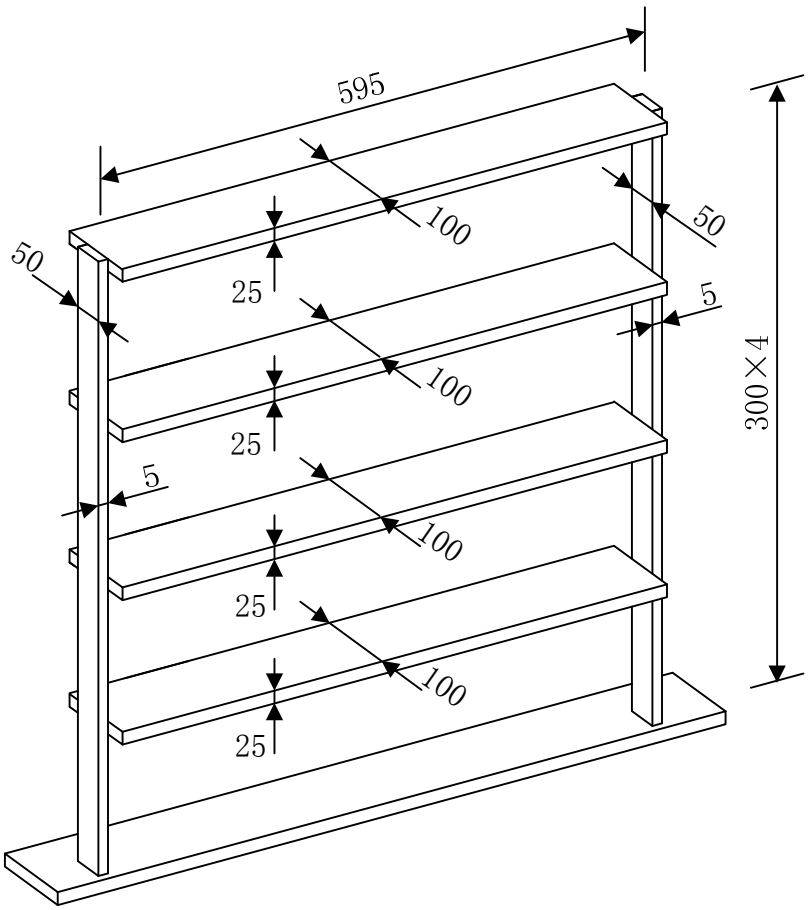

Figure 8 Dimensions of the frame (unit: mm)

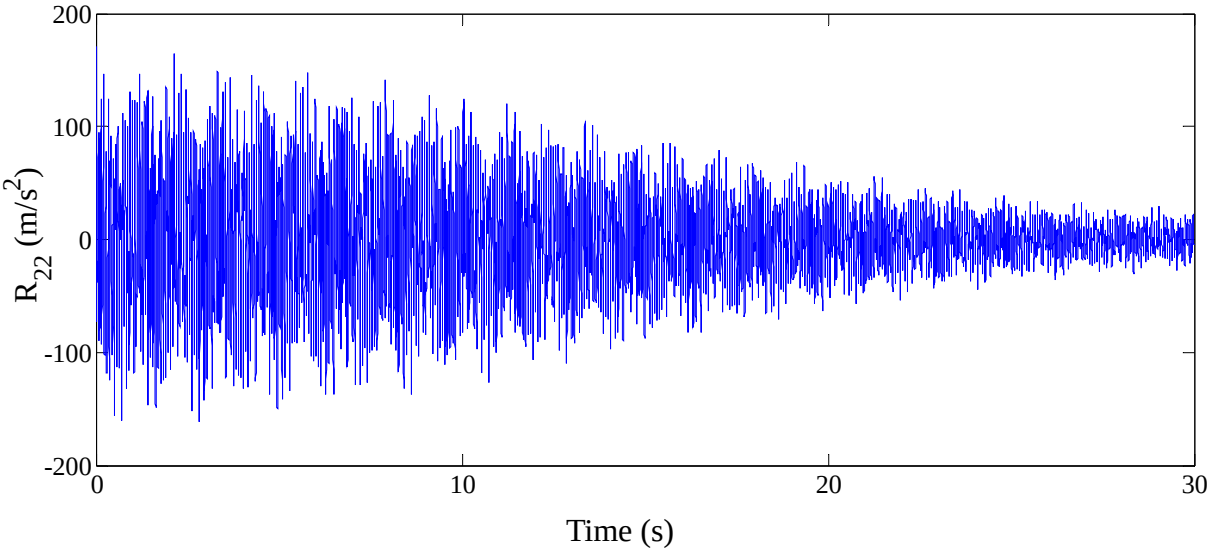

(a) Auto-correlation function $\boldsymbol{R}_{2,2}$

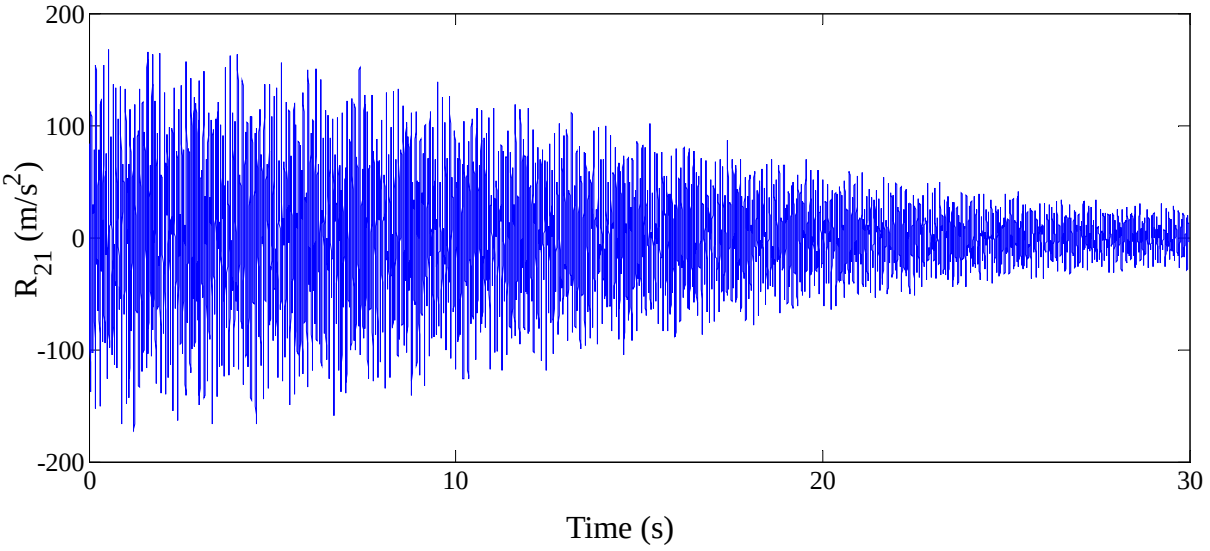

(b) Cross-correlation function $\boldsymbol{R}_{2,1}$

Figure 9 Auto- and cross-correlation functions

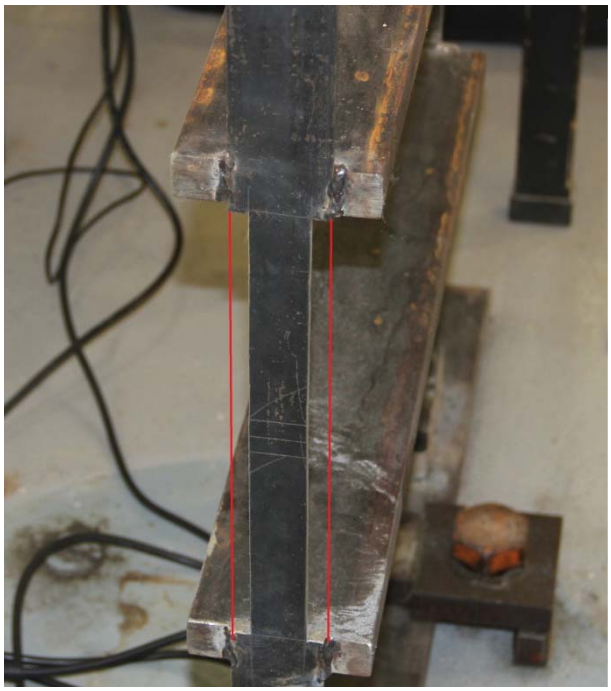

Figure 10 Damage of the frame

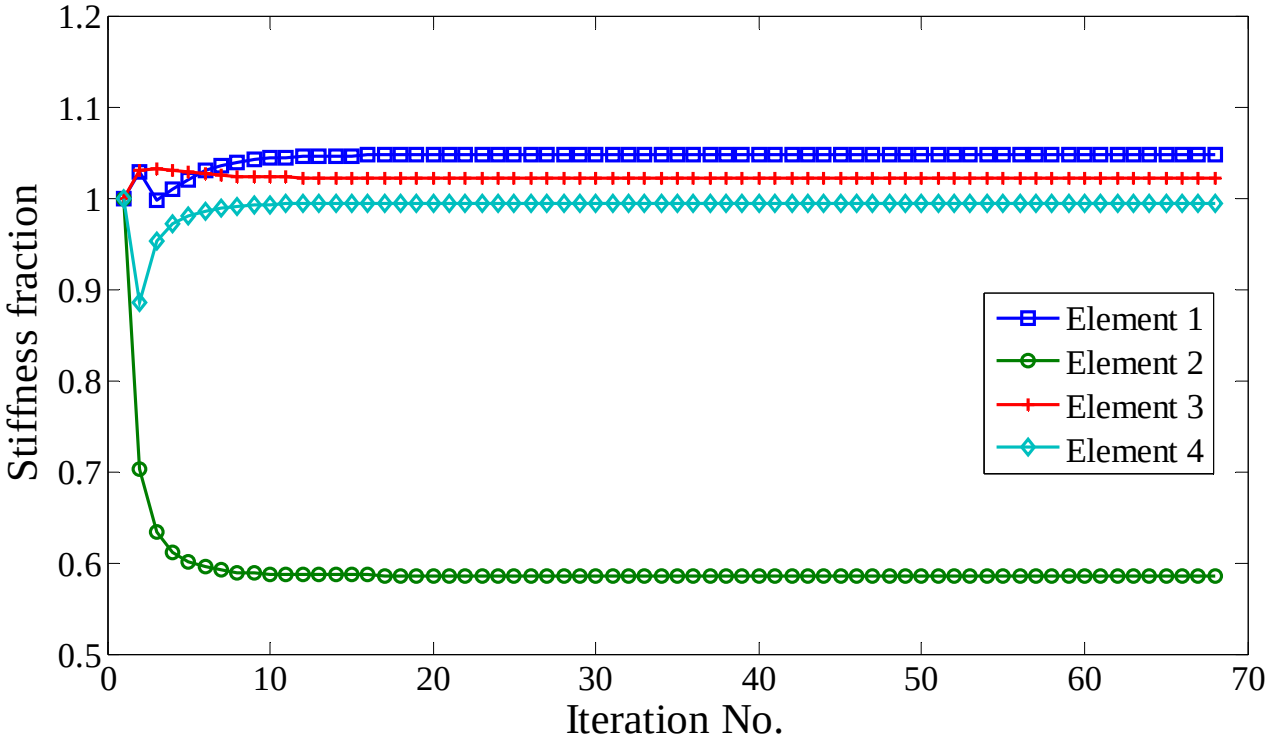

Figure 11 Iteration with identification results